frontiers | Frontiers in Immunology

TYPE Original Research
PUBLISHED 08 September 2025
DOI 10.3389/fimmu.2025.1587088

OPEN ACCESS

EDITED BY
Jesus Martinez-Barnetche,
National Institute of Public Health, Mexico

REVIEWED BY
José Luis Maravillas-Montero,
National Autonomous University of Mexico, Mexico
Laurence Menard,
Bristol Myers Squibb, United States

*CORRESPONDENCE
Ekaterina O. Serebrovskaya
katyaakts@gmail.com

†PRESENT ADDRESS
Evgenii V. Shchoka,
Information and Analysis Department, Federal State Budgetary Scientific Institution Research Centre for Medical Genetics, Moscow, Russia

‡These authors have contributed equally to this work

RECEIVED 03 March 2025
ACCEPTED 15 July 2025
PUBLISHED 08 September 2025

CITATION
Bryushkova EA, Shchoka EV, Lukyanov DK, Gikalo MB, Mushenkova N, Laktionov KK, Kazakov AM, Khalmurzaev OA, Matveev VB, Chudakov DM and Serebrovskaya EO (2025) FCRLs and atypical transcriptional pattern in tumor infiltrating B cells from lung and renal cancer. *Front. Immunol.* 16:1587088. doi: 10.3389/fimmu.2025.1587088

FCRLs and atypical transcriptional pattern in tumor infiltrating B cells from lung and renal cancer

Ekaterina A. Bryushkova[1,2‡], Evgenii V. Shchoka[2,3†‡], Daniil K. Lukyanov[1,2,4‡], Marina B. Gikalo[1,5], Natalya Mushenkova[1,6], Konstantin K. Laktionov[7], Alexey M. Kazakov[7], Oybek A. Khalmurzaev[7], Vsevolod B. Matveev[7], Dmitriy M. Chudakov[1,2,8] and Ekaterina O. Serebrovskaya[1,2,9*]

[1]Institute of Translational Medicine, Pirogov Russian National Research Medical University, Moscow, Russia, [2]Genomics of Adaptive Immunity Department, Shemyakin and Ovchinnikov Institute of Bioorganic Chemistry, Moscow, Russia, [3]School of Biological and Medical Physics, Dolgoprudny, Moscow region, Russia, [4]Center for Molecular and Cellular Biology, Moscow, Russia, [5]Moscow City Oncology Hospital №62, Moscow, Russia, [6]Unicorn Capital Partners, Moscow, Russia, [7]Federal State Budgetary Institution "N.N. Blokhin National Medical Research Center of Oncology" of the Ministry of Health of Russian Federation, Moscow, Russia, [8]Abu Dhabi Stem Cell Center, Abu Dhabi, United Arab Emirates, [9]Research and Development Department, Miltenyi Biotec B.V. & Co. KG, Bergisch Gladbach, Germany

Advances in high-dimensional flow cytometry and single-cell RNA sequencing (scRNA-seq) have enhanced our understanding of the heterogeneity of tumor-infiltrating B cells (TIBs). Subpopulations of TIBs exhibit diverse, sometimes opposing roles in tumor control, influenced by surface molecule, cytokine, and transcription factor expression. IgA and IgG expression in tumors have shown predictive value in melanoma and KRAS-mutated, but not KRAS wild-type, lung adenocarcinoma (LUAD). To investigate the functional differences between B cells producing these isotypes, we performed bulk transcriptome analysis of tumor-infiltrating surface-IgA+ (sIgA+) and sIgG+ memory B cells in LUAD. In LUAD, sIgA+ B cells overexpressed FCRL4, PDCD1, and RUNX2, suggesting an atypical chronically antigen-stimulated phenotype with features of exhaustion. Public scRNA-seq data revealed FCRL4-expressing TIBs as a distinct cluster with upregulation of genes involved in IFNγ and IFNα responses. sIgG+ B cells from LUAD overexpressed IL5RA, indicating a role for IL-5 in class-switch recombination to IgG. TCGA LUAD cohort analysis showed that the FCRL4/CD20 expression ratio correlates with lower survival, reinforcing FCRL4 as a marker of dysfunctional TIBs. Additionally, in renal cancer, high IGHA1/IGHG1 ratios were linked to worse survival. These findings suggest that the IgA/IgG ratio in tumors reflects not only the TME cytokine environment, but also functional differences in B cell populations, providing insights into their diverse roles in tumor progression.

KEYWORDS

tumor infiltrating B cells, surface IgA, lung adenocarcinoma, FcRL4, RUNX2

10.3389/fimmu.2025.1587088

Introduction

B cells may comprise more than 50% of lymphocyte infiltrate in tumors, thus being the important component of tumor microenvironment (TME) (1). Tumor-infiltrating B cells (TIBs) exhibit the hallmarks of antigen recognition, including somatic hypermutation, class switch recombination, clonal expansion and differentiation into antibody producing plasma cells (PCs) (2). In contrast to tumor-specific T cells that usually recognize mutated proteins (neoantigens), the target antigens of TIBs are predominantly self-proteins, thus B cells may complement the recognition pattern of T lymphocytes. All B cell subsets are found in human tumors, including activated B cells, memory and PCs, and even naive B cells.

Several reports studying the role of B cells in the context of non-small cell lung cancer (NSCLC) have shown that upregulation of B cell related genes (3), $CD20^+$ B cell infiltration (4), and the presence of B cell in tertiary lymphoid structures (TLS) correlated with patient survival, suggesting B cells role in tumor control. Approximately 50% of NSCLC patients have antibody reactivity to tumor antigens (5). Though anti-tumor activity of B cells is well characterized, in fact TIBs may play multiple roles in pro-tumoral antigen-specific immune responses as well. Immune promoting activities of TIBs include antigen presentation to T cells; direct cellular cytotoxicity (2), production of cytokines and antibodies. Depending on the isotype antibodies possess different effector functions. Tumor-specific antibodies may induce killing of tumor cells via ADCC (1, 6) and complement activation, enhance antigen capture and presentation by dendritic cells (7). Far fewer studies showed tumor promoting effects of antibodies, and mainly pro-tumoral activity of antibodies was attributed to the persistent immune complexes modulating the activity of Fc receptor-bearing myeloid cells (8).

Antibody isotypes may be associated with distinct functional B-cell populations. IgA isotype in some models characterizes suppressive intratumoral B cell population as was clearly shown *in vivo* in the murine model of metastatic prostate cancer (9, 10). The suppressive B cell (Breg) population was described as IgA^+CD19^+ plasmacytes expressing IL-10 and PD-L1 as well as other immunoregulatory factors. Bregs increased on chemotherapy and had a deleterious effect on tumoral CTL activation. The immunosuppressive IgA+TIBs are also relevant for clinical situation: based on the analysis of RNA-Seq data from TCGA, we have previously observed association of high IgA/IgG1 ratio with worse survival in melanoma patients (11) and bladder cancer patients receiving immunotherapy (11, 12). In case of lung adenocarcinoma (LUAD) low proportion of IgA among all intratumoral Ig was associated with improved overall survival in a specific subset of patients with mutated KRAS gene (13).

B cells may undergo exhaustion upon chronic antigen stimulation, a process analogous to T cell exhaustion (14–16). This process is defined as the progressive loss of functionality and reduced proliferative capability triggered by chronic antigen stimulation. Exhausted B cells (Bexh) are most studied in the context of chronic viral infection such as HIV, and have been defined as atypical memory B cells with downregulated CD21 and CD27 (14). Phenotype of HIV-induced Bexh includes higher expressions of certain chemokine receptors (CXCR3 and CCR6) and a number of ITIM-bearing receptors that serve as negative regulators of BCR-mediated activation, including FCRL4, FcγRIIB (CD32b), CD22, CD85d, and other B-cell inhibitory receptors, such as CD72, LAIR-1 and the programmed cell death 1 (PD-1) (14). Among ITIM-containing receptors FCRL4 was shown to be involved in maintenance of exhausted phenotype as its knockdown results in significant upregulation of BCR-dependent proliferation and cytokine response (16). Exhausted TIBs with $CD69^+HLA^-DR^+CD27^-CD21^-$ phenotype were identified in NSCLC patients and their presence positively correlated with the level of T regs in antigen presentation assay (17). At present the data on their characterization in lung cancer is scarce and no publications have been found studying possible association of this functional subpopulation with prognosis of survival.

FCRL4, together with FCRL5, was first identified as a marker of a distinct B cell population in human tonsils (18). FCRL4+FCRL5+ cell population was shown to have undergone more cell divisions compared to other B cell subpopulations, indicating stronger or longer BCR stimulation history. Functionally, it has been shown that FCRL4 recognizes J chain-linked IgA, and thus is a receptor for systemic IgA, but not mucosal secretory IgA (19). Upon IgA binding, ITIM domain downregulates BCR signaling, reducing proliferative response by recruiting SHP-1, -2 tyrosine phosphatases (20). Capable of not only dampening BCR signaling, but also enhancing TLR signaling, FCRL4 acts as a molecular switch between adaptive and innate immune response (21). In colorectal cancer, FCRL4 together with other B cell exhaustion markers, was associated with shorter overall survival (22). This study also showed that FCRL4 expression correlated with such B cell markers as CD19 and CD20, indicating association with overall B cell infiltration, whereas PD-L1 was correlated with T cell markers. On the other hand, FCRL4+FCRL5+ transcriptomic signature was associated with response to immunotherapy in lung cancer (23).

Better understanding and characterization of exhausted TIBs populations in different tumor contexts is needed, as well as more comprehensive insights into molecular mechanisms of B cell polarization. This understanding may give us new tools for modulation of complex immune-tumor interaction and tumor control. Here we present the results of comparative bulk RNA-seq transcriptome analysis of tumor-infiltrating IgA+ and IgG+ memory B cells in LUAD tumors, and perform a comprehensive analysis of scRNA-seq of TIBs in LUAD to reveal the molecular characteristics of exhausted B cell population.

Materials and methods

Human tumor specimens

A total of 8 samples of primary NSCLC were collected from NSCLC patients with stages I-III lung adenocarcinoma including

both KRASmut and KRASwt tumors. 11 samples of primary renal cancer were collected from patients with all stages of clear cell renal carcinoma, undergoing surgical resection. None of the patients received any anti-cancer therapy before tumor resection. Informed consent was obtained for each participant at the N.N.Blokhin cancer research center. The study was conducted in accordance with the Helsinki declaration.

Patient demographics and tumor histology can be found in Supplementary Tables S1 and S2.

No blinding or group randomization was conducted. No prior power analysis was conducted.

Tumor specimen processing

Tumor specimen were fragmented manually, incubated with 1 mg/ml of Liberase™ TL (Research Grade Roche, 5401020001) and 30 IU/ml DNAse I (Qiagen, 79254) in MACS Tissue storage solution (Miltenyi Biotec, 51606) and additionally homogenized with gentleMACS Dissociator (Miltenyi Biotec). Non-digestible tissue fragments were filtered with the 100-µm Cell Strainer (BD Falcon). Buffer EL (Qiagen 79217) was used for erythrocyte lysis and mononuclear cells were then separated with Ficoll-Paque™ PLUS (GE Healthcare, 17-1440-03). Single cell suspension in Versene solution with 5% human serum (Gemini Biotech) was additionally filtered with 70-µm Cell Strainer (SPL Lifesciences, 93040) to eliminate cell clumps and was subsequently used for antibody staining.

FACS sorting

B cell populations were sorted with FACSAria III (Becton Dickinson) in RLT (Qiagen). The following antibody panel was used: CD45-Alexa700 (BioLegend Cat# 304024, RRID: AB_493761), CD3-BrilliantViolet510 (BioLegend Cat# 300448, RRID: AB_2563468), CD19-FITC (Beckman Coulter Cat# A07768, RRID: AB_2924802), CD20-VioBlue (Miltenyi Biotec Cat# 130-094-167, RRID: AB_10830096), CD38-PerCP (BioLegend Cat# 303520, RRID: AB_893313), IgG1-PE (Cytognos CYT-IGG1PE, RRID: AB_3674600), IgA-Alexa647 (SouthernBiotech Cat# 2052-31, RRID: AB_2795711). Cells were sorted directly into the lysis buffer (RLT, Qiagen, 79216).

Bulk RNAseq library preparation

Total RNA was extracted using TRIzol reagent (15596–018, Ambion life technologies) according to the manufacturer's protocol, purified by AMPure-XP (Beckman Coulter, A63881). RNA pellet was dissolved in 40ul RNAse-free water (Qiagen), containing 4 IU/ul DNAseI (Qiagen, 79254) and 1 IU/ul RNAseq inhibitor (Recombinant RNAsin, Promega, N251B), and incubated for 15 min at 37°C. After DNAse treatment RNA was purified with AMPure-XP magnetic beads (Beckman Coulter) at a ratio of 1: 1. Reverse transcription and PCR amplification was performed using SMART-Seq v4 Ultra Low Input RNA Kit for Sequencing (TakaraBio, 634893).

RNAseq libraries were created using Nextera XT DNA Library Prep Kit (Illumina) with indexes Nextera XT Index Kit v2 (Illumina). The resulting libraries were sequenced with 150 bp paired-end reads on the Illumina HiSeq4000 sequencing system (Illumina Inc., San Diego).

Bulk RNA-seq data analysis

FastQC (RRID: SCR_014583) and MultiQC (RRID: SCR_014982) software was used to perform Quality Control (QC) of samples. The trimming of NexteraPE adapters, reads of low quality, and short reads was performed by Trimmomatic (RRID: SCR_011848).

The alignment of samples was performed using STAR (RRID: SCR_004463) with GRCh38.p13 genome assembly and GRCh38.109 gene annotation, filtering out multimappers. The quality of aligned reads was evaluated using Qualimap 2 (RRID: SCR_026258) software.

Gene quantification was performed using featureCounts from the Subread (RRID: SCR_009803) package. Resulting table of counts was used for differential expression (DE) analysis. Samples with zero counts, and samples with less than 50% reads aligned to exons were excluded.

Downstream analysis was done using the R programming language. Deconvolution method Xcell realized as a part of Immunedeconv (RRID: SCR_023869) package was used to exclude samples based on low level of B cell signature. For this method counts were transformed into transcripts per million (TPMs).

For DE analysis, a DESeq2 (RRID: SCR_015687) package was used. Genes for which there are less than three samples with normalized counts greater than or equal to 5 were filtered before DE analysis. Shrinkage of logarithmic fold changes (LFCs) was performed by function lfcShrink with Approximate Posterior Estimation for generalized linear model (apeglm) shrinkage estimator. To exclude correlation with isotype of B cells during further characterization, IGH, IGK, IGL, LOC, and JCHAIN genes were removed from the analysis. Adjusted p-value less than 0.01 and absolute LFC values greater than 1 were used as thresholds to identify and visualize DE genes. For volcano plot visualization top 20 upregulated and downregulated genes were labeled using geom_label_repel extension for the ggplot2 package. For visualization of genes using a heatmap only upregulated and downregulated genes were used.

Function class scoring (FCS) method gene set enrichment analysis (GSEA) was used for the interpretation of obtained results as a part of enrichplot package. For GSEA analysis, clusterProfiler package was used with parameters minimum gene set size = 25, maximum gene set = 500 and p-value cutoff = 0.05.

To assess the known and predicted protein interactions between target DEGs, package STRINGdb was used with parameter "medium confidence". Upregulated and downregulated genes were considered separately, as well as together.

Single-cell RNA seq data analysis

Processed cellranger-aligned 10X Chromium 3' scRNAseq data of immune cells from 35 NSCLC was obtained from effiken/Leader_et_al Github repository (24). The data was analyzed using the R programming language, most of the analysis was done via Seurat (RRID: SCR_016341) v4. To obtain high-quality scRNA-seq data, several filtering measures were applied to the raw matrix for each cell: the thresholds of maximum number of features < 4000, minimum number of features > 200, percent of mitochondrial RNA < 20, and percent of a ribosomal RNA > 5 were used. The dataset was processed by the use of the DoubletFinder (RRID: SCR_018771) package to identify clusters with doublets. To exclude biases during clustering at all stages, MALAT1, XIST, immunoglobulin, mitochondrial genes and genes involved in cell cycle were excluded from the list of variable genes. The first clusterization was produced using 2000 variable features, 40 dimensions and the resolution of 2.5. As a result of the first stage of clusterization, 4 clusters with 16389 cells were selected for downstream analysis based on non-plasma B cell marker expression (MS4A1 and CD19), excluding clusters marked as doublets according to DoubletFinder and clusters with expression of T cell, naive B cell and plasma cell markers (CD3E, CD8A, TCL1A (25), IGHD, CD38). The same procedure was also reproduced for samples from normal tissues from the same dataset, resulting in 2032 memory B cells from 28 patients.

Seurat algorithm of batch correction SelectIntegrationFeatures with parameter k.weight = 15, with the exclusion of immunoglobulin, mitochondrial, ribosomal and heat shock proteins (HSP) genes was used to account for differences between methods of library preparation of the samples. Downstream clustering and dimensional DE analysis was done with a min.pct parameter = 0.05 and minimal p_val_adj = 0.001. After clustering and DE, the cluster of interest was chosen based on a differentially expressed gene of interest: FCRL4. The GSEA function from clusterProfiler package and gseaplot function from enrichplot package were used for GSEA analysis and visualization. LFC values of DEGs of the 13th cluster were used for gene ranking. For the detailed scheme of scRNAseq data processing, see Supplementary Figure S1A. The quality of batch correction can be assessed on Supplementary Figure S1B.

TCGA data analysis

Most of the analysis was carried out using Gepia2 web server [Gene Expression Profiling Interactive Analysis 2 (RRID: SCR_026154)] (26).

For survival analysis split by stage, The Cancer Genome Atlas (RRID: SCR_003193) (TCGA) bulk tumor transcriptomic data (FPKM normalized) and clinical information of 478 LUAD patients and 515 KIRC patients were downloaded from the UCSC Xena (RRID: SCR_018938) (https://xenabrowser.net/) to study FCRL4 prognostic significance. To study the association of FCRL4 expressing B cells with OS, TCGA LUAD patients were split into high and low-FCRL4 groups based on the median cut-off value. The Kaplan–Meier method was employed for survival analysis, and the log-rank test was used to determine the statistical significance of the differences.

qPCR

For qPCR, we used amplified cDNA libraries generated by SMART-Seq v4 Ultra Low Input RNA Kit for Sequencing (see Bulk RNAseq library preparation step) with additional 10–11 cycles amplification. The obtained amplicons were quantified with Qubit fluorometer (Thermo Fisher) using dsDNA HS kit (Thermo Fisher). Concentrations were then adjusted to the same value for the qPCR step.

ABL1, GUSB, HPRT and TBP were selected as reference genes based on their levels of expression in the memory B-cells of lung adenocarcinoma patients.

Primers used for qPCR are summarized in Table 1.

qPCR was carried out in 25 µL reaction volume containing 1X qPCRmix-HS SYBR (Evrogen), 0.2 µM each primer, and 2ng/µL DNA template in a CFX96 Touch Real-Time PCR Detection System (BioRad). An initial denaturation and enzyme activation step of 2 minutes at 95°C was followed by amplification for 40 cycles at the following conditions: 15 seconds at 95°C, 30 seconds at 55.5°C, 30 seconds at 72°C. A final 5-minute extension at 72°C completed the protocol.

Melting curve analysis and the relative standard curve method performed in a CFX96 Touch Real-Time PCR Detection System (BioRad) equipped with CFX Manager™ Software (BioRad) and Precision Melt Analysis™ Software (BioRad) were used to ensure that the primers amplified the desired amplicons without forming dimers, and to calculate PCR efficiency and analytical sensitivity for each pair of primers.

Relative gene expression was calculated with the modified Pfaffl equation for multiple reference genes (https://toptipbio.com/qpcr-multiple-reference-genes/) using a custom Python script.

Code availability

Custom scripts used for data analysis is available through the following link: https://github.com/EvgeniyShchoka/Transcriptomics-Tumor-infiltrating-MemoryBCells/tree/master.

Results

Transcriptomic profiling of IgA and IgG expressing TIBs from lung and renal cancer

Tumor infiltrating B cells (TIBs) were isolated from 8 surgically excised stage I-II NSCLC tumors. All patients were

TABLE 1 Primers for qPCR.

Gene	Fwd	Rev	Reference/source
FCRL4	5'-AAAACTTAAGTACCAACTCTCCAAA-3'	5'-AATAAAACCTCTCTGCAAGGAGT-3'	(27).
FCRL5	5'-AGAACAAACTCCACCCTAATGTG-3'	5'-CCAAGAAGAGCCATTTTTCAGTTTG-3'	(27).
ABL1	5'-CTT CAG CGG CCA GTA GCA TCT-3'	5'- GTG ATT ATA GCC TAA GAC CCG G-3'	in-house
GUSB	5'-GCTCCGAATCACTATCGCCA-3'	5'-ACAGAAGTACAGACCGCTGC-3'	in-house
HPRT	5'-GGA CTA ATT ATG GAC AGG ACT GAA CGT-3'	5'- TCC ACA ATC AAG ACA TTC TTT CCA G-3'	in-house
TBP	5'-CGG AGA GTT CTG GGA TTG TA-3'	5'-GAC TGT TCT TCA CTC TTG GC-3'	in-house

treatment-naive to exclude any influence of previous therapy. Gating strategy based on CD45/CD19/CD20/CD38/CD3 was used to define B cell subpopulations such as plasma (CD45+CD3-CD19+CD20low/-CD38high) and B cells (CD45+CD3-CD19+ CD20highCD38low). B cells were further analyzed for IgA and IgG cell surface expression, and IgA/IgG-expressing B cells were defined as memory B cells (Bmem) based on their expression of class-switched BCRs. Experimental design is outlined in Figure 1. An example of B cell gating strategy is shown in Figure 2A.

The results of subpopulation analysis (Tables 2, 3, Figure 2B) revealed high patient-to-patient heterogeneity in the plasma to memory B cells ratio, as well as frequency of IgA and IgG-expressing Bmem cells. There was a trend for higher frequency of plasma cells in KRAS mutant tumors. IgA to IgG Bmem ratio varied from 0.3 to 15. Due to the limited number of patients it is impossible to make any conclusion about association of subpopulation frequencies and KRAS status of patients.

Target populations corresponding to memory B phenotype defined as CD45+/CD19+/CD20+/CD38-/CD3- with either IgA or IgG expression were sorted and used for bulk RNAseq library preparation.

DESeq2 was used to identify differentially expressed genes between IgA+ and IgG+ Bmem populations. Thresholds of log2FC > 1 and corrected p-value < 0.01 were used. After shrinkage with apeglm estimator, DE analysis has shown 46 DEGs between IgA+ and IgG+ TIBs populations, out of which 5 were upregulated in IgG TIBs, and 41 were upregulated in IgA TIBs (Figures 2C, D). Among the most upregulated genes in IgG high memory B cells in differential expression analysis (visualized as volcano plot, Figure 2C) were IL5Ra (log2FC = 1.19), CD200 (log2FC = =1.4), F13A1 (log2FC = 1.54), TAL2 (log2FC = 1.43), ZHX3 (log2FC = 1.23). IL5RA is a type-I transmembrane protein, responsible for the binding of immunostimulating cytokine Interleukin 5 (IL5). Pattern of IL5RA expression is in accordance with the known functional activity of IL-5/IL-5R axis in IgH class switch and production of IgG antibodies.

Gene set enrichment analysis showed that TNF, p53, MTORC1, interferon gamma, interferon alfa, IL2-STAT5 signaling pathways are enriched in sIgA-expressing TIBs in LUAD tumors (Figure 2E) as well as glycolysis, hypoxia and oxidative stress response pathways. mTOR and HIF1α belong to the central regulators of immune cells energy metabolism, important for shaping the immune response (28). Nutrient-limited microenvironment in the tumor niche drives B cell metabolic adaptation that may result in their functional polarization. TOR is a known inducer of HIF1α, which explains the coordinated upregulation of mTOR-HIF1α pathways. Consequently, HIF1 triggers transcriptional responses to limited oxygen and mediates the expression of genes encoding glucose transporters and glycolytic enzymes, thus shifting energy metabolism towards glycolysis as an adaptation to hypoxic conditions and increased energy demands (28). HIF1α is known to function in a stage-specific manner to regulate B lymphocyte differentiation and proliferation.

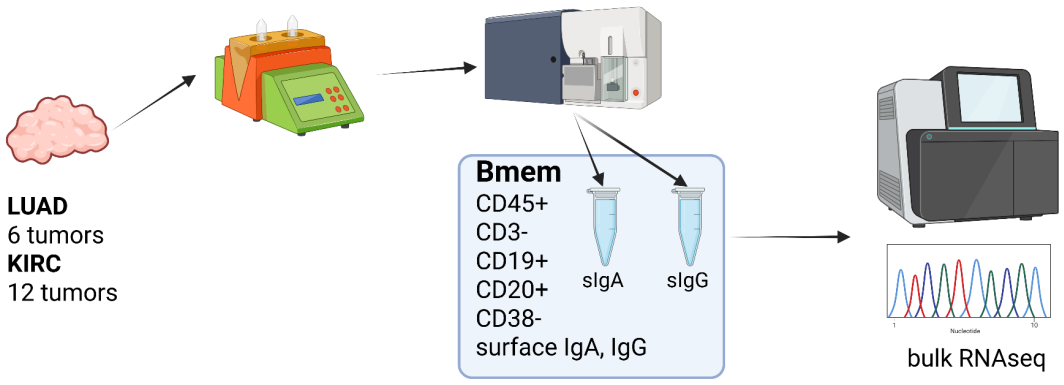

FIGURE 1
Transcriptomic profiling of surface IgA and IgG expressing TIBs, overall experimental design (Created in https://BioRender.com).

On the other hand, sIgG-expressing TIBs show enrichment in RNA processing, ribosome biogenesis, and other pathways related to protein synthesis.

FCRL4 and associated transcriptional factor RUNX2 identified as overexpressed in IgA-expressing tumor-infiltrating B-cells in lung cancer

FCRL4 has been identified among genes most upregulated in IgA expressing memory TIBs. FCRL4 is a member of Fc Receptor-Like proteins (FCRL), that is able to bind soluble immunoglobulins via the Fc-domain. FCRL4 expression was previously shown to be restricted to a subpopulation of Bmem cells with a distinctive phenotype and tissue localization pattern (29, 30). FCRL4 interacts with polymeric IgA (and to a significantly lesser extent to IgG3 and IgG4) (19), its intracellular domain contains three consensus immunoreceptor tyrosine-based inhibition motifs (ITIMs), and co-ligation of FCRL4 with the BCR aborts BCR-mediated signaling (20). The expression of FCRL4 was shown to correlate with transcription factor runt-related transcription factor 2 (RUNX2) (31), which is also upregulated in IgA-expressing B cells in our data (adjusted p-value = 7.36e-05, LFC = -1.65). RUNX2 gene was also shown to be specifically upregulated in CD27(-)IgA (+) B cells, a distinct mucosal Bmem population producing polyreactive anti-commensal antibodies (32). In our data RNAseq, RUNX2 was upregulated in 2 out of 3 sIgA-expressing TIB samples where FCRL4 was also upregulated (Figures 3A, C). Expression of FCRL4in individual TIB samples from our cohort was further validated using qPCR and found to be significantly enriched in IgA vs IgG-expressing TIBs from LUAD (Figure 3B). IL5RA, on

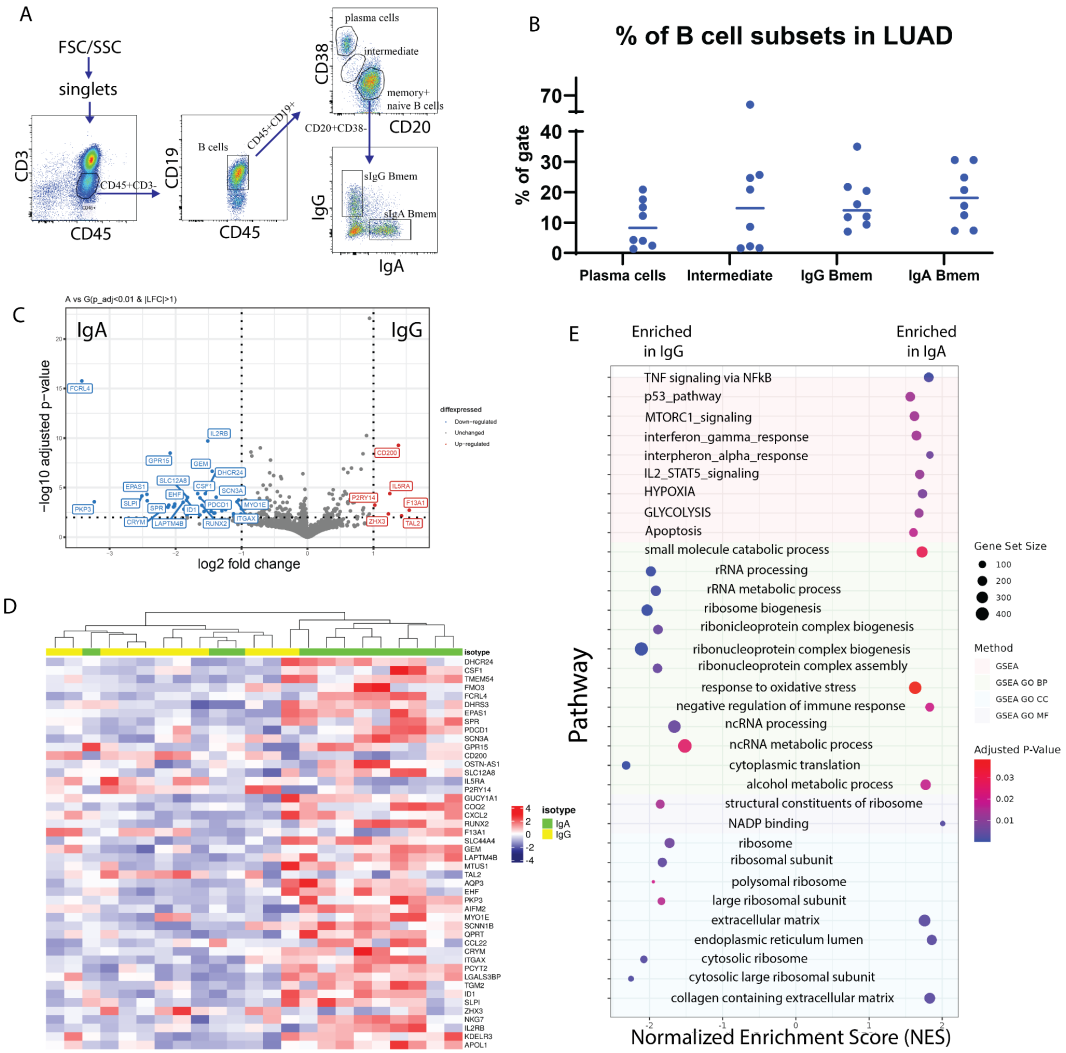

FIGURE 2
Transcriptomic profiling of surface IgA and IgG expressing TIBs LUAD. **(A)** Flow cytometry analysis of TILs subpopulations from a representative LUAD patient (lc-p17). Subpopulations of T lymphocytes (CD45+CD3+), B lymphocytes (CD45+CD3-CD19+), plasma cells (CD20lowCD38high), (naive + memory) B cells (CD20highCD38low), IgA- and IgG-expressing memory B cells are indicated. **(B)** Percentage of the B cell subpopulations across samples. **(C)** Volcano plot representing differentially expressed genes in IgA Bmem (left) and IgG Bmem (right). **(D)** Heatmap representing all differentially expressed genes. **(E)** Gene set enrichment analysis of DE genes from panel **(D)**.

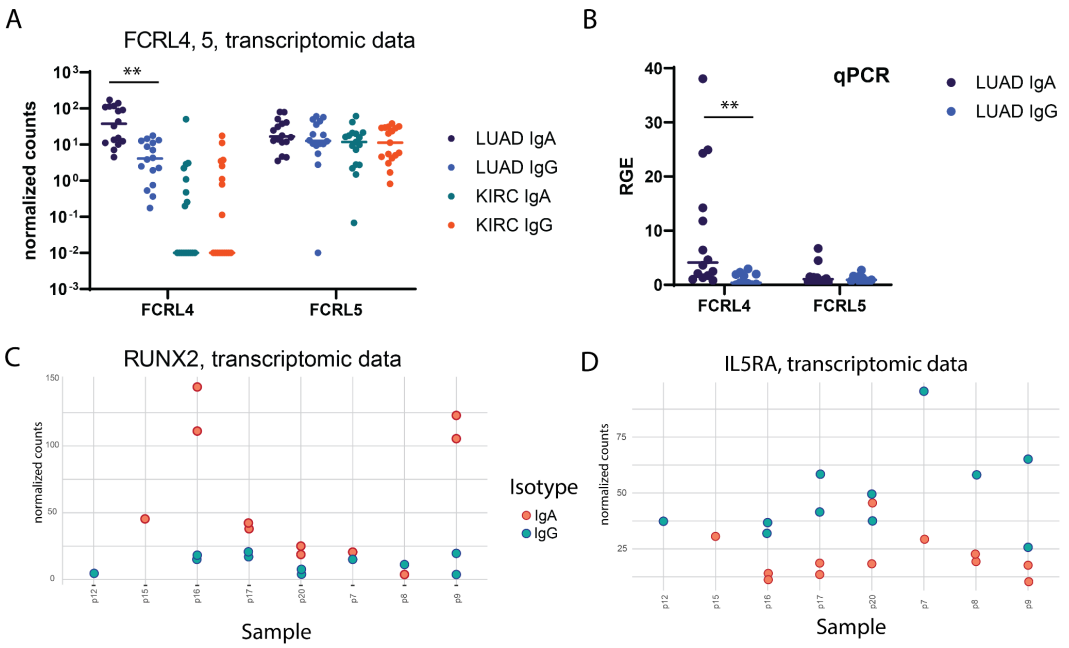

FIGURE 3
Verification of differential gene expression findings. **(A)** per-sample distribution of expression (normalized counts, transcriptomic data) for FCRL4 gene in LUAD samples (unpaired Mann-Whitney test with Bonferroni correction). **(B)** Relative gene expression of FCRL4 and FCRL5 in LUAD samples quantified by qPCR analysis (unpaired Mann-Whitney test with Bonferroni correction). **(C, D)** per-sample distribution of expression (normalized counts) for RUNX2 and IL5RA genes in LUAD samples (transcriptomic data). For every panel - 2 technical replicates from each patient are represented as separate datapoints.

the other hand, was upregulated in the majority of sIgG-expressing TIB samples from our cohort (Figure 3D).

FCRL4 expression normalized to total B cell infiltration is associated with decreased survival in lung cancer, but not renal cancer

The cancer genome atlas (TCGA) was used to analyze possible association between increased presence of FCRL4 among Bmem cells and survival of lung adenocarcinoma and kidney carcinoma (KIRC) patients. First, we analyzed how FCRL4 expression correlated with other immune cell markers in LUAD and KIRC samples from the TCGA database, using GEPIA2 server (26) (Figure 4A). In KIRC, no significant correlation was observed with CD3, CD8, CD19 or CD20, and the expression of FCRL4 was overall very low. In LUAD samples, FCRL4 expression correlated well with CD20 (R=0.73) and CD19 (R=0.76). Also, in LUAD samples, expression of FCRL4 was significantly higher in tumor samples, compared to the matched normal tissue (Figure 4B). In KIRC samples, FCRL4 expression was low both in tumor and matched normal tissue samples. These observations, in conjunction with our own RNAseq data, indicate that FCRL4-

TABLE 2 Subpopulation composition of TIBs from LUAD patients.

Patient	KRAS status	Plasma cells (%)	B cells (%)	IgA-expressing Bmem (%)	IgG-expressing Bmem (%)
lc-p7	unknown	22,5	70	29	23,5
lc-p8	wt	1,8	94,2	19	15,3
lc-p9	wt	12,8	83,7	7,3	35
lc-p12	wt	5,1	78	11,8	10,5
lc-p15	wt	5,4	67	7,8	10,7
lc-p16	wt	5,7	13	2	7,2
lc-p17	G12C	14,6	42	21	9,7
lc-p20	G12C	9,3	63,9	8,9	18,3

TABLE 3 Subpopulation composition of TIBs from KIRC patients.

Patient	Plasma cells (%)	B cells (%)	IgA-expressing Bmem (%)	IgG-expressing Bmem (%)
rc-p12	13,5	63,3	71	5
rc-p16	32,8	8	12	8
rc-p17	0,8	20	20,7	11
rc-p18	14	72	16,6	16,9
rc-p19	3,4	75,5	5,0	1,4
rc-p20	48	18	13	21
rc-p21	4	10,7	20,3	12,6
rc-p22	11	77	8,4	7
rc-p23	3,6	89,7	10,7	36
rc-p25	16,1	69,4	1,4	1,7
rc-p26	0,65	95	0,5	12,7

expressing B cells infiltrate LUAD tumors and may be functionally relevant for tumor progression. Therefore, we then performed survival analysis on the TCGA LUAD and KIRC cohorts using GEPIA2 server (Figure 4C). Unnormalized FCRL4 expression weakly correlated with longer survival in LUAD (HR=0.72, p(HR) =0.035), whereas FCRL4 normalized to the expression of MS4A1 (CD20) correlated with poor survival prognosis (HR=1.8, p(HR) =0.00013). This observation suggests that whereas infiltration with B cells (reflected in total unnormalized FCRL4 expression) was a weakly positive factor, higher proportion of FCRL4-expressing B cells represented a negative factor, probably related to the higher degree of B cells exhaustion and involvement of negative feedback mechanisms of BCR signaling. In KIRC, survival data were not representative, due to low FCRL4 expression. Survival correlation with FCRL4 expression was statistically significant in Stage II LUAD patients, p=0.0046 (Figure 4D).

FCRL4 expressing cells form a distinct cluster in tumor-infiltrating memory B cells from lung cancer, that is characterized by interferon signaling genes, antigen presentation signature and exhaustion signature

To verify the findings of our analysis of bulk RNAseq data obtained from sorted IgA and IgG TIBs from lung cancer, and also from the analysis of TCGA RNAseq data, we performed analysis of a scRNAseq dataset from Leader et al. (24). As the original dataset contained CD45 positive LUAD immune cells, we filtered the data by subpopulation-specific marker expression to represent cells with memory B cell phenotype, and then performed batch effect correction and integration of data from different donors using Seurat CCA integration pipeline (33) (Supplementary Figures S1A-E).

The panel of classical B-cell markers suggests biologically relevant clusters of CD27+ memory B cells: group of IGHM+ unswitched clusters (1, 9), class-switched clusters (clusters 2, 3, 6, 8, 13), and class-switched clusters with remaining IGHM expression (0, 4, 5, 7, 11) (Supplementary Figure S1E). Cluster 9 may belong to CR2 (CD21) high resting memory population. The marginal zone B cells (CDC1A+) did not form a cluster in this dataset.

We identified a cluster (cluster 13 on Figures 5A, B) comprising 347 cells with the upregulated expression of FCRL4 (Log2FC = 1.42) relative to other clusters. FCRL4+ memory B cell cluster also has shown elevated expression of interferon response signature genes, which includes ISG15, IFIT3, IFI44L, MX2, OAS1 genes (Figure 5E). Other notable genes overexpressed in this cluster include ITGAX, PDCD1, TNFSF11 and FAS (Figure 5C), as well as genes associated with antigen presentation - CD83, CD86 and MHCII (Figure 5E).

ITGAX is often found in combination with other markers in the panels defining exhaustion (see (14, 34)). TNFSF11 (RANKL) was also found in FCRL4-expressing B cells in the context of autoimmunity, in the population defined as pro-inflammatory and probably contributing to RA pathogenesis (35). Upregulation of FAS (CD95), alongside loss of CD21, was identified as a marker of B-cell dysfunction in HIV-infected individuals (36), contributing to B cell apoptosis (37).

The CD83 gene is significantly upregulated in the FCRL4-positive cluster, although not exclusively in it. The exact functions and biology of CD83 protein remain largely unknown and are actively studied as it is a clinically relevant immune checkpoint (38). In activated B cells and dendritic cells, membrane bound CD83 is thought to stabilize the expression of MHC II and CD86 via the negative regulation of MARCH1. In accordance with this, we find that MHC II genes and CD86 are upregulated in cluster 13 compared with other clusters (Figure 5E). It was also previously shown that soluble form of CD83 promoted immunosuppression in several autoimmune conditions, restricting effector CD4 T cells and promoting Treg differentiation and proliferation. We note that both

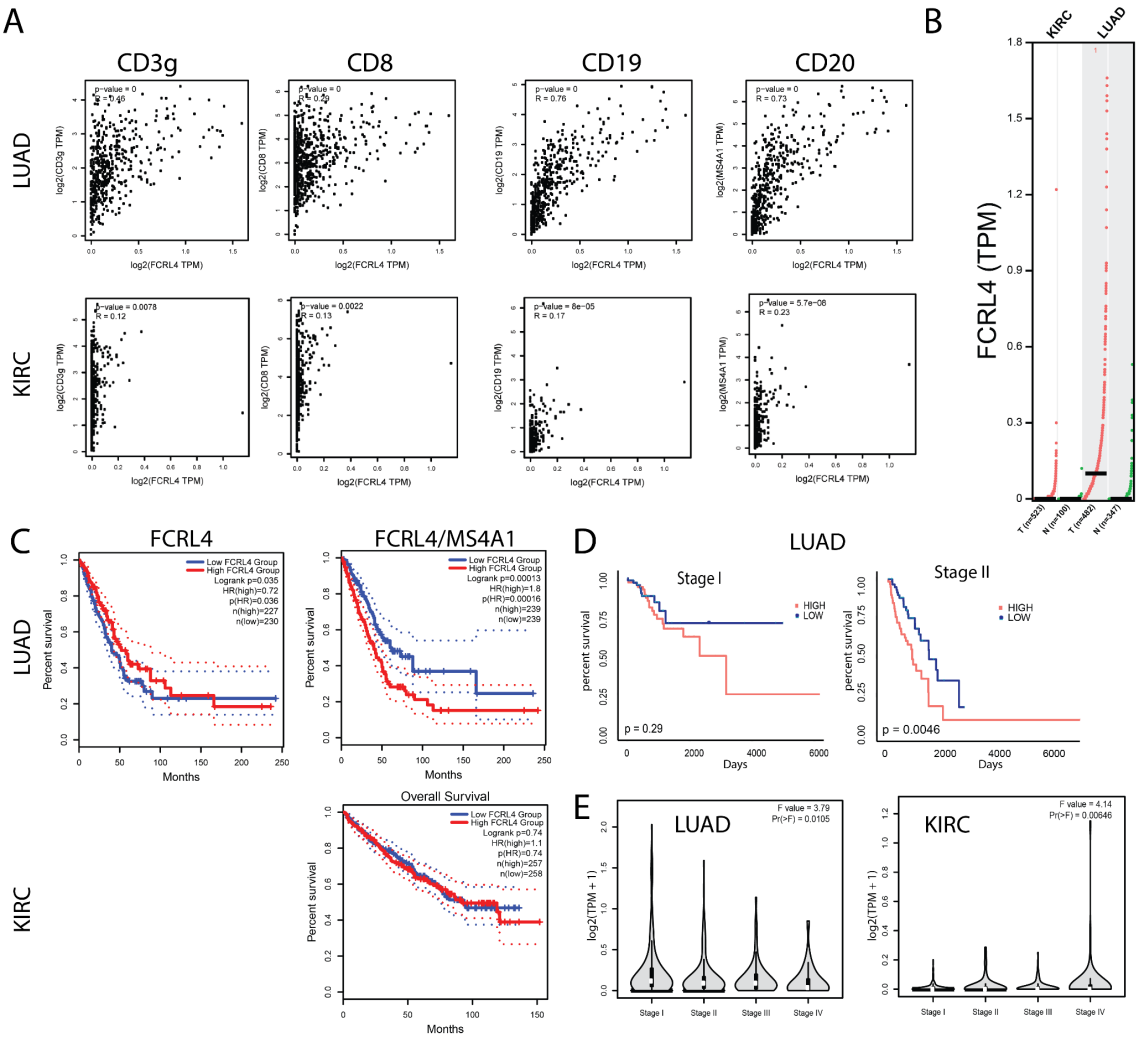

FIGURE 4
FCRL4 gene expression correlates with B cell marker expression and with patient survival. **(A)** correlation of FCRL4 expression with CD3γ, CD8, CD19 and CD20 in LUAD and KIRC samples from TCGA database. **(B)** FCRL4 is overexpressed in LUAD, but not in KIRC tumors versus normal tissue samples (N = 523(KIRC tum), 100 (KIRC norm), 482 (LUAD tum), 347 (LUAD norm). **(C)** In LUAD, unnormalized FCRL4 expression positively correlates with survival (LUAD: HRhigh = 0.72, p(HR) = 0.035), whereas FCRL4 expression normalized to B cell marker MS4A1 (CD20) (FCRL/CD20) negatively correlates with survival (LUAD: HRhigh = 1.8, p(HR) = 0.0013, KIRC: not significant). **(D)** For stage I LUAD, correlation of FCRL4/CD20 with patient survival is statistically insignificant (p = 0.29), whereas for stage II FCRL4/CD20 negatively correlates with survival (p = 0.0046). **(E)** stage plots for FCRL4 expression in LUAD and KIRC. TCGA data was analyzed using the GEPIA2 server 26 **(A-C, E)**.

of these modes of action can potentially limit antitumor immune response, adding to the protumorigenic role of FCRL4+ tumor-infiltrating memory B cells.

We performed gene set enrichment analysis for DEGs of cluster 13, and found that IFNγ and IFNα response, IL2-STAT5, TNFa and mTORC1 signaling pathways were enriched (Figure 5D). These pathways were also found to be enriched in surface IgA-expressing memory B cells from our RNA-seq data. Another set of enriched GO terms for cluster 13 DEGs is related to antigen processing and presentation via MHC class II.

Significant proportion of cluster 13 cells were found to express none or both IGHG1 and IGHA1 at comparable levels. Gating the cells according to expression of IGHA1 and IGHG1 results in roughly the same proportions of single positive IgA/IgG cells across the clusters of memory B cells (Supplementary Figure S1D). It seems to be a general issue with isotype expression in scRNAseq memory B cell data, as in a paper by Fitzsimons et al. (39), which included pan-cancer intratumoral B cell data from 15 different datasets, widespread coexpression of IGHA1 and IGHG1 in Bmems was also found. Thus, despite the overrepresentation of IgA-expressing cells, this limitation makes it challenging to attribute this cluster to either IgA or IgG-switched B cells. FCRL4 upregulation appears to be a tumor-specific feature, as according to the scRNA-seq data from the normal lung tissue from the same dataset, FCRL4 is not expressed by any cluster (Supplementary Figure S2). The study also contains CITE-seq data, however, only five B-cell relevant genes were included in the panel, IgG1 and IgA not being among them. Overall, scRNAseq data corroborates bulk RNAseq data and paints a more detailed portrait of the FCRL4+ B cell subset in LUAD.

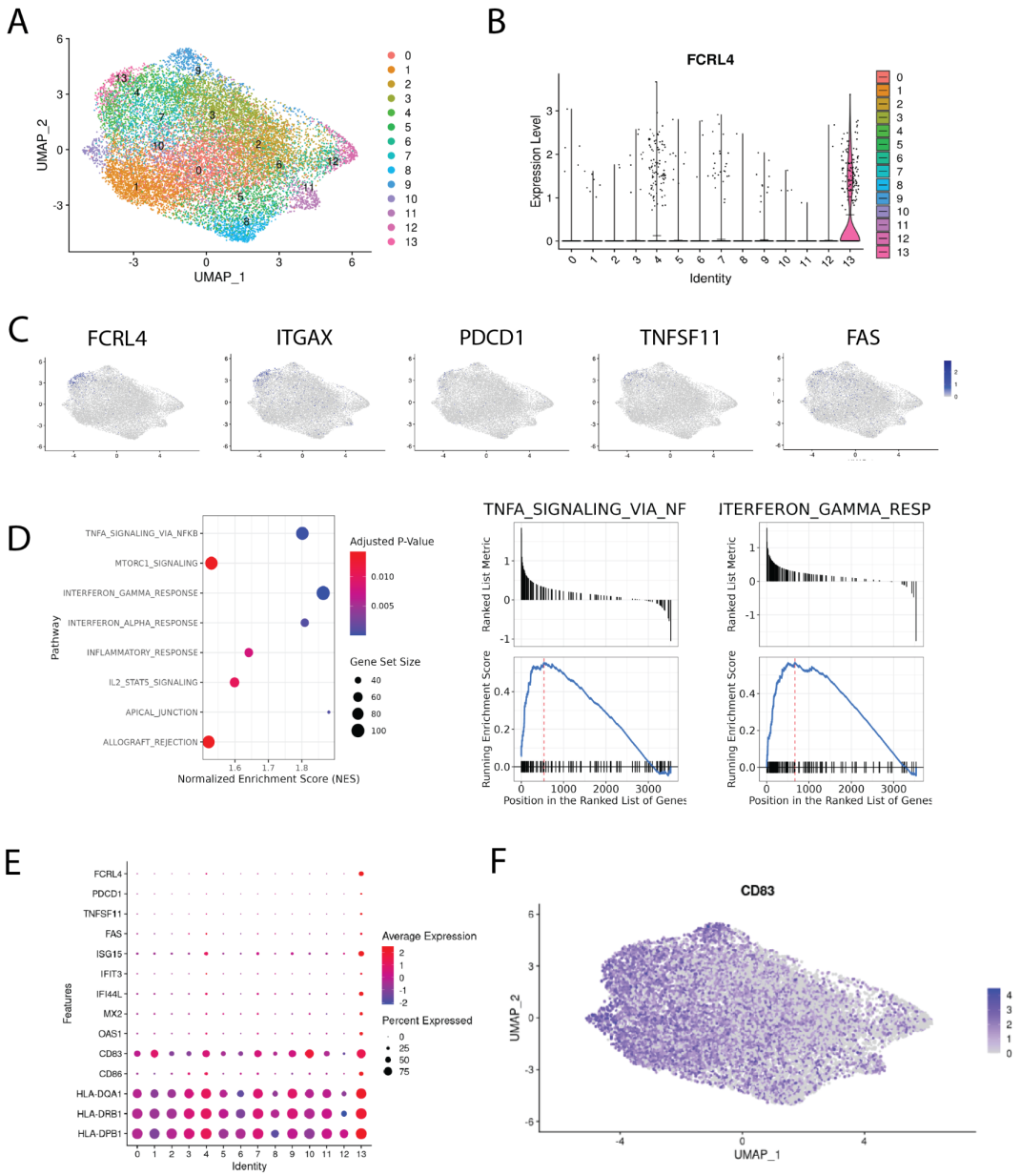

FIGURE 5
Single-cell transcriptomic analysis of memory B cells infiltrating NSCLC tumors. **(A)** integrated Bmem dataset from 24. A. Uniform manifold approximation and projection (UMAP) representation of memory B cells after data integration, colors correspond to scRNAseq clusters; **(B)** violin plot of FCRL4 expression across clusters, means are shown as black lines; **(C)** chosen genes overexpressed in FCRL4 cluster, mapped to the UMAP representation; **(D)** GSEA analysis of DEGs from FCRL4-overexpressing cluster 13; **(E)** dotplot of gene expression for several cluster 13 markers across the dataset; **(F)** UMAP representation of CD83 expression across the dataset;.

Low FCRL5 and high IGHA1/IGHG1 ratio correlate with prolonged survival in KIRC

To evaluate the role of B cell infiltration in renal cancer, we performed survival analysis for B cell markers on TCGA RNAseq data from KIRC samples using GEPIA2 server (Figures 6A-D). All markers of B cell infiltration, including CD19, IGHA1, IGHG1, normalized to CD45, correlate with shorter overall survival, which is not the case in LUAD (Figures 6E-H). Most surprisingly, the high ratio of IGHA1 to IGHG1 very strongly correlated with prolonged survival (Figure 6I) in renal cancer. As isotype switching to IgA isotype is influenced by TGFβ, we hypothesized that high IgA/IgG ratio may be an indicator of TGFβ-rich microenvironment. However, neither TGFβ alone, nor TGFβ/MS4A1, nor TGFβ/CD45 ratio showed similar correlation with survival, as IgA/IgG ratio (data not shown). Also, as opposed to LUAD, high FCRL5 expression in KIRC correlated strongly with worse survival (Figure 6J).

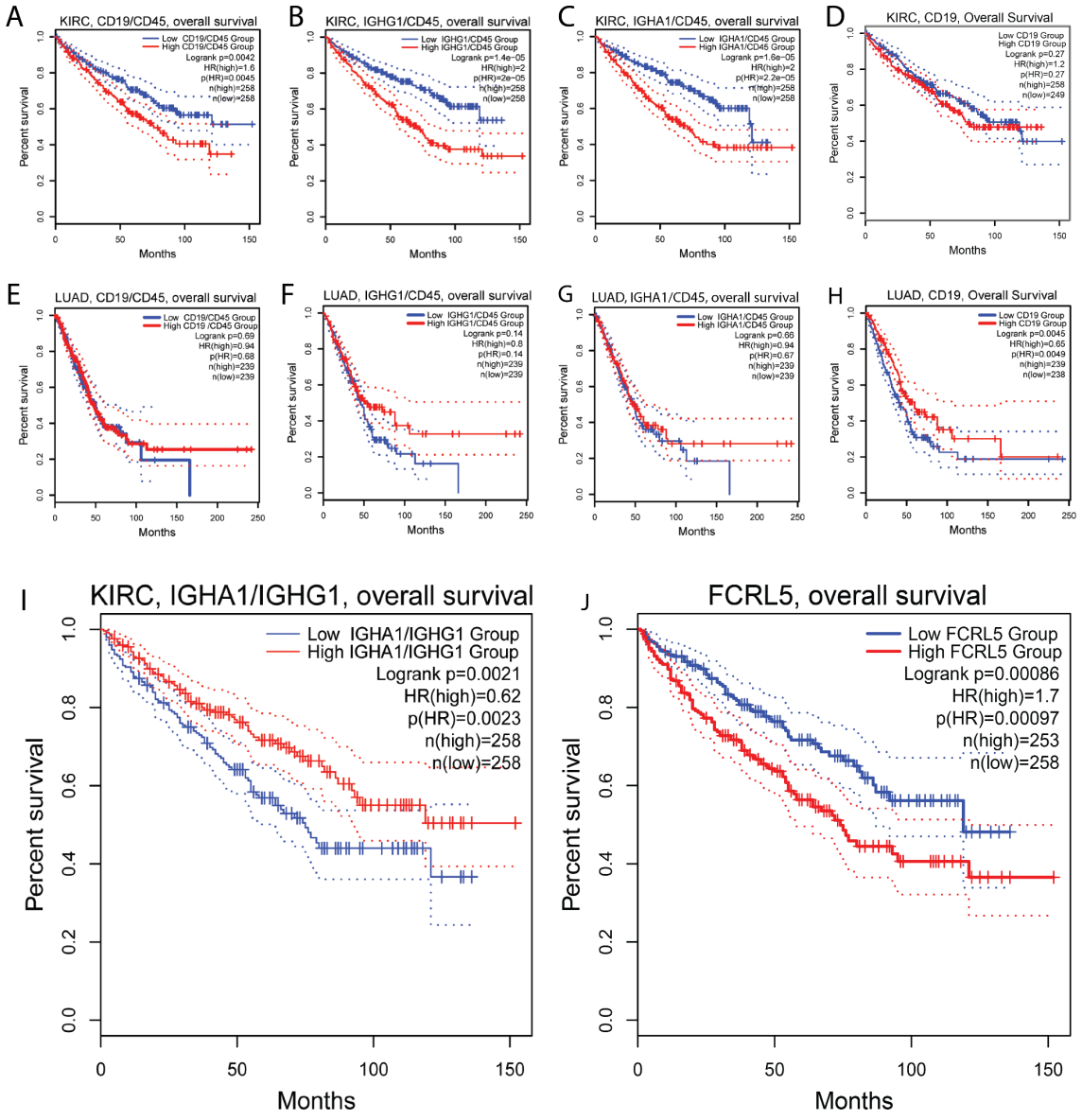

FIGURE 6
Association of B cell markers and immunoglobulin expression with survival in renal clear cell carcinoma. **(A-D)** Ratio of CD19/CD45 **(A)**, IGHG1/CD45 **(B)**, IGHA1/CD45 **(C)** are negatively associated with survival in renal cell carcinoma, indicating overall negative role of B cells in renal cancer. **(E–H)** In LUAD, no association with survival was found for ratio of CD19/CD45 **(E)**, IGHG1/CD45 **(F)**, IGHA1/CD45 **(G)**; **(I)** high ratio of IGA1 to IGHG1 is positively associated with survival in renal cell carcinoma. **(J)** low FCRL5 expression is positively associated with survival in renal cell carcinoma.

Discussion

The majority of recent TME research has focused on the molecular profiling of tumor-infiltrating T cells, with significantly less emphasis on the phenotypic diversity of B cells. However, it is increasingly recognized that B cells are a key component of the intratumoral immune landscape. Specific B cell subpopulations in the TME of various cancers may influence the tumor immune infiltrate, promoting either pro-tumoral or antitumoral functional profiles. B cells can amplify anti-tumor immune responses through antibody production and ADCC/ADCP. However, if they differentiate into regulatory or exhausted phenotypes, their effector function is diminished (40). Cell exhaustion, defined as a dysfunctional state caused by chronic antigenic overstimulation, has been observed in various lymphocyte populations (41). It is characterized by increased expression of inhibitory receptors, abnormal chemokine and adhesion ligand/receptor expression, and weak proliferative responses to various stimuli (Summarized for B cells in Table 4).

In this study we did not identify any chemokines or adhesion molecules differentially expressed between IgA and IgG memory B cell (Bmem) populations. However, we found upregulation of two inhibitory receptors - FCRL4 and PDCD1 (PD-1) - in IgA+ B cells in lung adenocarcinoma (LUAD). Expression of FCRL4 marks the population of exhausted tissue-like memory (TLM) B-cells previously described in HIV-infected individuals (16). FCRL4

downregulates B-cell receptor (BCR) signaling by inhibiting BCR-mediated calcium mobilization, tyrosine phosphorylation of several intracellular proteins, and activation of protein kinase pathways (20). Similarly, FCRL5 inhibits B cell activation via SHP-1 tyrosine phosphatase recruitment (42).

Considering that FCRL4 is a receptor for soluble IgA (19), the following negative feedback mechanism may be proposed: overactivated IgA-class-switched Bmem cells sense the local IgA level via upregulated FCRL4 receptor and downregulate BCR signaling. In our current study we did not specifically measure soluble IgA production by the cells sorted as sIgA+/sIgG+ cells with our gating strategy, and it is not possible to distinguish between soluble and membrane IgA based on transcriptomic data, so currently we are unable to discriminate between autocrine and paracrine mechanisms, or a combination of both. To our knowledge, this is the first time upregulation of FCRL4 molecules in sIgA-expressing Bmem cells has been reported. We aimed to also confirm this finding with scRNA-seq analysis, but this was not possible due to technical constraints. To further explore this question, it would be beneficial to combine scRNAseq with CITE-Seq to label surface IgG/IgA, which could resolve the issue of ambiguous mapping of immunoglobulin isotypes in scRNA-seq data.

In addition to FCRL4, other markers possibly associated with B-cell exhaustion were upregulated in the IgA+ Bmem population, including PD-1, which aligns well with the B-cells exhaustion pattern described previously in chronic infections (14).

Previously, Bexh, along with exhausted T and NK cells, were found in colorectal carcinoma (CRC) samples (22), where high expression of FCRL4, as well as other exhaustion genes, was significantly associated with worse prognosis independently of tumor's molecular subtype. The overall survival (OS) of patients bearing CRC with high FCRL4 expression was more than three times shorter compared to patients with low expression. Combination of high FCRL4 and high CD20 expression was also associated with shorter OS. FCRL4+FCRL5+ Bmem population was previously identified in naïve NSCLC patients undergoing neoadjuvant immune checkpoint blockade (ICB) + chemotherapy (23). In these FCRL4+ cells interferon-stimulated genes (CCR1, STAT1, and GBP4) and co-stimulatory molecules (CD86, CD40L) were highly expressed. Based on their gene expression profile, TLS localization and association with better prognosis and response to immunotherapy, this B cell subpopulation was proposed to possess potential anti-tumor activity that was released by ICB therapy. FCRL4+FCRL5+ B cell signature was also a good prognostic factor in melanoma (23). Interestingly, IFNα and tumor necrosis factor (TNF) were predicted as possible drivers of FCRL4+FCRL5+ phenotype. Similarly, in our study we also observed enrichment of IFN and TNF signaling in the FCRL4-overexpressing B cell subpopulation. Immune activation proceeds in parallel with the induction of negative feedback mechanisms, which, in case of chronic inflammation, can become predominant and contribute to immune dysfunction. Type I interferons induce many of the suppressive factors that limit immunity (43), and one effect of IFNs may be the upregulation of programmed death-ligand 1 (PD-L1), which aligns well with the observed PD-1^{high} phenotype of FCRL4+ B cells (43).

TABLE 4 Phenotypic characterization of Bexh population.

Condition	Bexh phenotype	Ref
HIV infection	CD19+CD10−CD27−CD21low	(44)
	FCRL4 high CD20highCD27−CD21low Siglec-6+, CD32b high, CD22 high; CD85d high CD72 high, LAIR-1 high, **PD-1 high**	(16)
	CD85+ **CD11c (ITGAX) high**, CXCR3 high, CCR6high, CD62 low, CXCR4 low, CXCR5 low, CCR7 low	(14)
	CD95+	(36)
Graft-versus-host disease	CD85+	(15)
Plasmodium falciparum infection	CD85j high, CD22 high, **CD11c (ITGAX) high**, CXCR3 high; CXCR4 high, **FCRL4 high**, CD62L low, CXCR5low, CCR7low	(34)
Colorectal cancer	***FCRL4***+, *SIGLEC2+, SIGLEC6, CD19+CD20+CD79a+*	(22)
NSCLC	CD69+HLA−DR+CD27−CD21-	(17)

Genes identified in the current work highlighted in bold.

Our current study further confirms the potential utility of FCRL4 as a prognostic marker, when used in combination with other B cell markers, and also as a potential therapeutic target. We demonstrated that FCRL4 expression, normalized to the expression of CD20, correlates with poor survival outcomes in LUAD. In KIRC, however, survival data were not conclusive, due to overall low FCRL4 expression. Furthermore, in LUAD, we observed inverse correlation between FCRL4 expression and clinical stage. According to The Cancer Genome Atlas (TCGA) data, LUAD tumor progression was accompanied by a decrease in FCRL4 levels, whereas renal carcinoma showed a substantial increase in FCRL4 expression as the tumor progressed from stage I to stage IV. Since FCRL4 upregulation may represent a mechanism of B cells autoregulation by circulating antibodies, we suggest that increased expression of FCRL4 indicates an active humoral response. Conversely, its decrease during tumor progression may indicate the selection of low-immunogenic tumor variants that evade effective humoral control. Notably, there is a reported trend in NSCLC patients for decreased autoantibody responses in the course of tumor progression. An analysis of the humoral response to a panel of seven autoantigens (TP53, c-Myc, HER2, NY-ESO-1, CAGE, MUC1, and GBU4) in NSCLC patients revealed that 71-100% had elevated antibody levels to at least one of the antigens (45), with the highest frequencies observed at earlier stages. A similar trend was observed for anti-TOP2A and anti-ACTR3 antibodies, which showed a significant decrease in positivity from early to late tumor stages (43-50% vs. 22-24%) (46).

Class-switch recombination to IgA isotype is induced by TGFβ (47), an immunosuppressive cytokine produced by tumor cells, as well as by various cellular components of tumor stroma and

immune infiltrate. NSCLC TME is characterized by the abundance of cancer-associated fibroblasts producing TGFB1 (48) and frequency of IgA+ cells was found to positively correlate with frequency of Tregs and exhausted CD8 T cells. Similarly, Bruno et al. showed that exhausted TIBs were associated with a regulatory (FoxP3+CD4+) TIL response in co-culture experiments (17). On the causal side, TIBs, including Bexh, may actively contribute to the conversion of T cells into a regulatory phenotype by presenting antigens to CD4+ TILs in the immunosuppressive, TGFβ-rich environment. Therefore, possible association of FCRL4+ IgA+ Bmem with Treg infiltration, as well as the degree of T cell exhaustion, presents an important avenue for future research.

Identified pattern of genes upregulated together with FCRL4 overlaps with the list of differentially expressed genes in FCRL4+ Bmem from human tonsils, with RUNX2 and IL2RB identified in both studies. Runx2 belongs to a family of transcriptional factors described in the context of early hematopoiesis and thymopoiesis (40). In the hematopoietic system, RUNX2 has been studied mostly in plasmacytoid dendritic cells (pDCs), in which RUNX2 facilitated pDC homeostasis and anti-viral responses. Recent data suggest participation of Runx2 in functional differentiation of T cells (Tfh, CD8 T mem) (49–51). Though increased RUNX2 expression is associated with various B cell-derived malignancies, including myeloma, B-cell lymphoma and acute lymphoblastic leukemia, evidence for RUNX2 role in TIBs is lacking. FCRL4 promoter contains eight potential RUNX binding sites (31). RUNX2 dependent regulation of FCRL4 has not been confirmed in reporter experiments, their failure may be explained by the absence of right co- factor transfection, thus the question of RUNX2-dependent regulation of FCRL4 needs adequate investigation. IL2RB represents the beta subunit of IL-2 receptor that is present in high and intermediate affinity receptor types. IL2 is a well-known T cell pro-proliferative cytokine. In human B lymphocytes it was shown to imprint naive B cell fate towards plasma cell differentiation (34).

In this work we gained additional evidence in line with the previous reports that IgA- and IgG-class-switched B cells differ in their functional polarization and may have distinct roles in TME, important for tumor progression and survival prognosis. Our work also further supports the view that an autocrine negative feedback loop on immunoglobulin production develops throughout the course of tumor development, downregulating the activity of the B cells involved in the antitumor immune response through the interaction of inhibitory FCRLs with immunoglobulins these B cells produce. These findings may open new avenues for research in TIBs biology, and for development of innovative immunotherapeutic strategies.

Data availability statement

The datasets presented in this study can be found in online repositories. The names of the repository/repositories and accession number(s) can be found below: https://www.ncbi.nlm.nih.gov/geo/, GSE287504.

Ethics statement

The studies involving humans were approved by ethics committee of the N.N.Blokhin cancer research center. The study was conducted in accordance with the Helsinki declaration. The studies were conducted in accordance with the local legislation and institutional requirements. The participants provided their written informed consent to participate in this study.

Author contributions

EB: Investigation, Methodology, Project administration, Writing – original draft. ES: Formal analysis, Investigation, Software, Visualization, Writing – original draft. DL: Investigation, Methodology, Software, Visualization, Writing – original draft. MG: Investigation, Methodology, Writing – original draft. NM: Writing – original draft. KL: Methodology, Resources, Writing – review & editing. AK: Project administration, Resources, Writing – review & editing. OK: Project administration, Resources, Writing – review & editing. VM: Resources, Writing – review & editing. DC: Funding acquisition, Supervision, Writing – review & editing. ES: Investigation, Methodology, Supervision, Writing – original draft, Writing – review & editing.

Funding

The author(s) declare financial support was received for the research and/or publication of this article. Supported by the Ministry of Health of the Russian Federation.

Conflict of interest

Author NM was employed by the company Unicorn Capital Partners. Current affiliation of author ES is Miltenyi Biotec.

The remaining authors declare that the research was conducted in the absence of any commercial or financial relationships that could be construed as a potential conflict of interest.

Generative AI statement

The author(s) declare that no Generative AI was used in the creation of this manuscript.

Publisher's note

All claims expressed in this article are solely those of the authors and do not necessarily represent those of their affiliated organizations, or those of the publisher, the editors and the

reviewers. Any product that may be evaluated in this article, or claim that may be made by its manufacturer, is not guaranteed or endorsed by the publisher.

Supplementary material

The Supplementary Material for this article can be found online at: https://www.frontiersin.org/articles/10.3389/fimmu.2025.1587088/full#supplementary-material

SUPPLEMENTARY TABLE 1
Patient characteristics - lung cancer.

SUPPLEMENTARY TABLE 2
Patient characteristics - renal cancer.

SUPPLEMENTARY FIGURE 1
(A) Diagram representing the scRNAseq data analysis steps. **(B)** Histogram of clusters split by sample of origin to assess the efficiency of batch effect removal. **(C)** Dotplot of B-cell subpopulation marker gene expression across 13 Bmem clusters. **(D)** Histogram of the IGHA1/IGHG1 isotype expression across the clusters. The cells with the zero expression of one of IGHA1/IGHG1 were considered single-positive. **(E)** B cell subpopulation marker gene expression mapped to UMAP representation of Bmem from LUAD tumors..

SUPPLEMENTARY FIGURE 2
Expression of major genes of interest mapped to the UMAP representation of memory B cells from the normal lung tissue.

References

1. Hu Q, Hong Y, Qi P, Lu G, Mai X, Xu S, et al. Atlas of breast cancer infiltrated B-lymphocytes revealed by paired single-cell RNA-sequencing and antigen receptor profiling. *Nat Commun*. (2021) 12:2186. doi: 10.1038/s41467-021-22300-2

2. Laumont CM, Banville AC, Gilardi M, Hollern DP, Nelson BH. Tumour-infiltrating B cells: immunological mechanisms, clinical impact and therapeutic opportunities. *Nat Rev Cancer*. (2022) 22:414–30. doi: 10.1038/s41568-022-00466-1

3. Mount DW, Putnam CW, Centouri SM, Manziello AM, Pandey R, Garland LL, et al. Using logistic regression to improve the prognostic value of microarray gene expression data sets: application to early-stage squamous cell carcinoma of the lung and triple negative breast carcinoma. *BMC Med Genomics*. (2014) 7:33. doi: 10.1186/1755-8794-7-33

4. Al-Shibli KI, Donnem T, Al-Saad S, Persson M, Bremnes RM, Busund L-T, et al. Prognostic effect of epithelial and stromal lymphocyte infiltration in non-small cell lung cancer. *Clin Cancer Res*. (2008) 14:5220–7. doi: 10.1158/1078-0432.CCR-08-0133

5. Germain C, Gnjatic S, Tamzalit F, Knockaert S, Remark R, Goc J, et al. Presence of B cells in tertiary lymphoid structures is associated with a protective immunity in patients with lung cancer. *Am J Respir Crit Care Med*. (2014) 189:832–44. doi: 10.1164/rccm.201309-1611OC

6. Kurai J, Chikumi H, Hashimoto K, Yamaguchi K, Yamasaki A, Sako T, et al. Antibody-dependent cellular cytotoxicity mediated by cetuximab against lung cancer cell lines. *Clin Cancer Res*. (2007) 13:1552–61. doi: 10.1158/1078-0432.CCR-06-1726

7. Carmi Y, Spitzer MH, Linde IL, Burt BM, Prestwood TR, Perlman N, et al. Allogeneic IgG combined with dendritic cell stimuli induce antitumour T-cell immunity. *Nature*. (2015) 521:99–104. doi: 10.1038/nature14424

8. Barbera-Guillem E, May KF Jr., Nyhus JK, Nelson MB. Promotion of tumor invasion by cooperation of granulocytes and macrophages activated by anti-tumor antibodies. *Neoplasia*. (1999) 1:453–60. doi: 10.1038/sj.neo.7900054

9. Shalapour S, Lin X-J, Bastian IN, Brain J, Burt AD, Aksenov AA, et al. Inflammation-induced IgA+ cells dismantle anti-liver cancer immunity. *Nature*. (2017) 551:340–5. doi: 10.1038/nature24302

10. Shalapour S, Font-Burgada J, Di Caro G, Zhong Z, Sanchez-Lopez E, Dhar D, et al. Immunosuppressive plasma cells impede T-cell-dependent immunogenic chemotherapy. *Nature*. (2015) 521:94–8. doi: 10.1038/nature14395

11. Bolotin DA, Poslavsky S, Davydov AN, Frenkel FE, Fanchi L, Zolotareva OI, et al. Antigen receptor repertoire profiling from RNA-seq data. *Nat Biotechnol*. (2017) 35:908–11. doi: 10.1038/nbt.3979

12. Dyugay IA, Lukyanov DK, Turchaninova MA, Serebrovskaya EO, Bryushkova EA, Zaretsky AR, et al. Accounting for B-cell behavior and sampling bias predicts anti-PD-L1 response in bladder cancer. *Cancer Immunol Res*. (2022) 10:343–53. doi: 10.1158/2326-6066.CIR-21-0489

13. Isaeva OI, Sharonov GV, Serebrovskaya EO, Turchaninova MA, Zaretsky AR, Shugay M, et al. Intratumoral immunoglobulin isotypes predict survival in lung adenocarcinoma subtypes. *J Immunother Cancer*. (2019) 7:279. doi: 10.1186/s40425-019-0747-1

14. Moir S, Ho J, Malaspina A, Wang W, DiPoto AC, O'Shea MA, et al. Evidence for HIV-associated B cell exhaustion in a dysfunctional memory B cell compartment in HIV-infected viremic individuals. *J Exp Med*. (2008) 205:1797–805. doi: 10.1084/jem.20072683

15. Khoder A, Alsuliman A, Basar R, Sobieski C, Kondo K, Alousi AM, et al. Evidence for B cell exhaustion in chronic graft-versus-host disease. *Front Immunol*. (2017) 8:1937. doi: 10.3389/fimmu.2017.01937

16. Kardava L, Moir S, Wang W, Ho J, Buckner CM, Posada JG, et al. Attenuation of HIV-associated human B cell exhaustion by siRNA downregulation of inhibitory receptors. *J Clin Invest*. (2011) 121:2614–24. doi: 10.1172/JCI45685

17. Bruno TC, Ebner PJ, Moore BL, Squalls OG, Waugh KA, Eruslanov EB, et al. Antigen-presenting intratumoral B cells affect CD4+ TIL phenotypes in non-small cell lung cancer patients. *Cancer Immunol Res*. (2017) 5:898–907. doi: 10.1158/2326-6066.CIR-17-0075

18. Li H, Dement-Brown J, Liao P-J, Mazo I, Mills F, Kraus Z, et al. Fc receptor-like 4 and 5 define human atypical memory B cells. *Int Immunol*. (2020) 32:755–70. doi: 10.1093/intimm/dxaa053

19. Liu Y, Goroshko S, Leung LYT, Dong S, Khan S, Campisi P, et al. FCRL4 is an fc receptor for systemic igA, but not mucosal secretory igA. *J Immunol*. (2020) 205:533–8. doi: 10.4049/jimmunol.2000293

20. Ehrhardt GRA, Davis RS, Hsu JT, Leu C-M, Ehrhardt A, Cooper MD, et al. The inhibitory potential of Fc receptor homolog 4 on memory B cells. *Proc Natl Acad Sci U S A*. (2003) 100:13489–94. doi: 10.1073/pnas.1935944100

21. Sohn HW, Krueger PD, Davis RS, Pierce SK. FcRL4 acts as an adaptive to innate molecular switch dampening BCR signaling and enhancing TLR signaling. *Blood*. (2011) 118:6332–41. doi: 10.1182/blood-2011-05-353102

22. Sorrentino C, D'Antonio L, Fieni C, Ciummo SL, Di Carlo E. Colorectal cancer-associated immune exhaustion involves T and B lymphocytes and conventional NK cells and correlates with a shorter overall survival. *Front Immunol*. (2021) 12:778329. doi: 10.3389/fimmu.2021.778329

23. Hu J, Zhang L, Xia H, Yan Y, Zhu X, Sun F, et al. Tumor microenvironment remodeling after neoadjuvant immunotherapy in non-small cell lung cancer revealed by single-cell RNA sequencing. *Genome Med*. (2023) 15:14. doi: 10.1186/s13073-023-01164-9

24. Leader AM, Grout JA, Maier BB, Nabet BY, Park MD, Tabachnikova A, et al. Single-cell analysis of human non-small cell lung cancer lesions refines tumor classification and patient stratification. *Cancer Cell*. (2021) 39:1594–1609.e12. doi: 10.1016/j.ccell.2021.10.009

25. Stewart A, Ng JC-F, Wallis G, Tsioligka V, Fraternali F, Dunn-Walters DK, et al. Single-cell transcriptomic analyses define distinct peripheral B cell subsets and discrete development pathways. *Front Immunol*. (2021) 12:602539. doi: 10.3389/fimmu.2021.602539

26. Tang Z, Kang B, Li C, Chen T, Zhang Z. GEPIA2: an enhanced web server for large-scale expression profiling and interactive analysis. *Nucleic Acids Res*. (2019) 47:W556–60. doi: 10.1093/nar/gkz430

27. Sullivan RT, Kim CC, Fontana MF, Feeney ME, Jagannathan P, Boyle MJ, et al. FCRL5 delineates functionally impaired memory B cells associated with plasmodium falciparum exposure. *PloS Pathog*. (2015) 11:e1004894. doi: 10.1371/journal.ppat.1004894

28. FranChina DG, Grusdat M, Brenner D. B-cell metabolic remodeling and cancer. *Trends Cancer Res*. (2018) 4:138–50. doi: 10.1016/j.trecan.2017.12.006

29. Ehrhardt GRA, Hsu JT, Gartland L, Leu C-M, Zhang S, Davis RS, et al. Expression of the immunoregulatory molecule FcRH4 defines a distinctive tissue-based population of memory B cells. *J Exp Med*. (2005) 202:783–91. doi: 10.1084/jem.20050879

30. Falini B, Tiacci E, Pucciarini A, Bigerna B, Kurth J, Hatzivassiliou G, et al. Expression of the IRTA1 receptor identifies intraepithelial and subepithelial marginal zone B cells of the mucosa-associated lymphoid tissue (MALT). *Blood*. (2003) 102:3684–92. doi: 10.1182/blood-2003-03-0750

31. Ehrhardt GRA, Hijikata A, Kitamura H, Ohara O, Wang J-Y, Cooper MD, et al. Discriminating gene expression profiles of memory B cell subpopulations. *J Exp Med*. (2008) 205:1807–17. doi: 10.1084/jem.20072682

32. Berkowska MA, Schickel J-N, Grosserichter-Wagener C, de Ridder D, Ng YS, van Dongen JJM, et al. Circulating human CD27-igA+ Memory B cells recognize

bacteria with polyreactive igs. *J Immunol*. (2015) 195:1417–26. doi: 10.4049/jimmunol.1402708

33. Stuart T, Butler A, Hoffman P, Hafemeister C, Papalexi E, Mauck WM, et al. Comprehensive integration of single-cell data. *Cell*. (2019) 177:1888–1902.e21. doi: 10.1016/j.cell.2019.05.031

34. Weiss GE, Crompton PD, Li S, Walsh LA, Moir S, Traore B, et al. Atypical memory B cells are greatly expanded in individuals living in a malaria-endemic area. *J Immunol*. (2009) 183:2176–82. doi: 10.4049/jimmunol.0901297

35. Yeo L, Lom H, Juarez M, Snow M, Buckley CD, Filer A, et al. Expression of FcRL4 defines a pro-inflammatory, RANKL-producing B cell subset in rheumatoid arthritis. *Ann Rheumatol Dis*. (2015) 74:928–35. doi: 10.1136/annrheumdis-2013-204116

36. Sciaranghella G, Tong N, Mahan AE, Suscovich TJ, Alter G. Decoupling activation and exhaustion of B cells in spontaneous controllers of HIV infection. *AIDS*. (2013) 27:175–80. doi: 10.1097/QAD.0b013e32835bd1f0

37. Samuelsson A, Sönnerborg A, Heuts N, Cöster J, Chiodi F. Progressive B cell apoptosis and expression of Fas ligand during human immunodeficiency virus type 1 infection. *AIDS Res Hum Retroviruses*. (1997) 13:1031–8. doi: 10.1089/aid.1997.13.1031

38. Grosche L, Knippertz I, König C, Royzman D, Wild AB, Zinser E, et al. The CD83 molecule - an important immune checkpoint. *Front Immunol*. (2020) 11:721. doi: 10.3389/fimmu.2020.00721

39. Fitzsimons E, Qian D, Enica A, Thakkar K, Augustine M, Gamble S, et al. A pan-cancer single-cell RNA-seq atlas of intratumoral B cells. *Cancer Cell*. (2024) 42:1784–1797.e4. doi: 10.1016/j.ccell.2024.09.011

40. Mirlekar B, Wang Y, Li S, Zhou M, Entwistle S, De Buysscher T, et al. Balance between immunoregulatory B cells and plasma cells drives pancreatic tumor immunity. *Cell Rep Med*. (2022) 3:100744. doi: 10.1016/j.xcrm.2022.100744

41. Roe K. NK-cell exhaustion, B-cell exhaustion and T-cell exhaustion-the differences and similarities. *Immunology*. (2022) 166:155–68. doi: 10.1111/imm.v166.2

42. Haga CL, Ehrhardt GRA, Boohaker RJ, Davis RS, Cooper MD. Fc receptor-like 5 inhibits B cell activation via SHP-1 tyrosine phosphatase recruitment. *Proc Natl Acad Sci*. (2007) 104:9770–5. doi: 10.1073/pnas.0703354104

43. Snell LM, McGaha TL, Brooks DG. Type I interferon in chronic virus infection and cancer. *Trends Immunol*. (2017) 38:542–57. doi: 10.1016/j.it.2017.05.005

44. Amu S, Ruffin N, Rethi B, Chiodi F. Impairment of B-cell functions during HIV-1 infection. *AIDS*. (2013) 27:2323–34. doi: 10.1097/QAD.0b013e328361a427

45. Chapman CJ, Murray A, McElveen JE, Sahin U, Luxemburger U, Türeci O, et al. Autoantibodies in lung cancer: possibilities for early detection and subsequent cure. *Thorax*. (2008) 63:228–33. doi: 10.1136/thx.2007.083592

46. Pei L, Liu H, Ouyang S, Zhao C, Liu M, Wang T, et al. Discovering novel lung cancer associated antigens and the utilization of their autoantibodies in detection of lung cancer. *Immunobiology*. (2020) 225:151891. doi: 10.1016/j.imbio.2019.11.026

47. Dedobbeleer O, Stockis J, van der Woning B, Coulie PG, Lucas S. Cutting edge: active TGF-β1 released from GARP/TGF-β1 complexes on the surface of stimulated human B lymphocytes increases class-switch recombination and production of igA. *J Immunol*. (2017) 199:391–6. doi: 10.4049/jimmunol.1601882

48. Chung JY-F, Chan MK-K, Li JS-F, Chan AS-W, Tang PC-T, Leung K-T, et al. TGF-β Signaling: from tissue fibrosis to tumor microenvironment. *Int J Mol Sci*. (2021) 22(14):7575. doi: 10.3390/ijms22147575

49. Vaillant F, Blyth K, Andrew L, Neil JC, Cameron ER. Enforced expression of Runx2 perturbs T cell development at a stage coincident with beta-selection. *J Immunol*. (2002) 169:2866–74. doi: 10.4049/jimmunol.169.6.2866

50. Choi J, Diao H, Faliti CE, Truong J, Rossi M, Bélanger S, et al. Bcl-6 is the nexus transcription factor of T follicular helper cells via repressor-of-repressor circuits. *Nat Immunol*. (2020) 21:777–89. doi: 10.1038/s41590-020-0706-5

51. Olesin E, Nayar R, Saikumar-Lakshmi P, Berg LJ. The transcription factor runx2 is required for long-term persistence of antiviral CD8+ Memory T cells. *Immunohorizons*. (2018) 2:251–61. doi: 10.4049/immunohorizons.1800046